

**Remarks on recent results on neutron production during thunderstorms**

A. Chilingarian,\* N. Bostanjyan, T. Karapetyan, and L. Vanyan  
*Yerevan Physics Institute, Alikhanyan Brothers 2, Yerevan 000036, Armenia*  
 (Received 24 June 2012; published 13 November 2012)

We analyze the neutron fluxes correlated with thunderstorm activity recently measured at mountain altitudes by the Tien-Shan, Tibet, and Aragats groups. We perform simulations of the photonuclear reactions of gamma rays born in the electron-gamma ray avalanches and calculate the expected count rates of the neutron detectors used by the three groups. We also present results of an independent experiment performed at the Nor Amberd high altitude research station in Armenia. Our analysis supports the Tibet and Aragats groups' conclusions on the photonuclear nature of thunderstorm-correlated neutrons (directly in the neutron monitor and in the atmosphere). The photonuclear reactions of the gamma rays born in the electron-photon avalanches in the thunderstorm atmospheres interacting with the air atoms and with lead producer of a neutron monitor can provide neutron yield compatible with additional count of neutron monitors registered during thunderstorm ground enhancements.

DOI: [10.1103/PhysRevD.86.093017](https://doi.org/10.1103/PhysRevD.86.093017)

PACS numbers: 92.60.Pw, 13.40.-f, 94.05.Dd

**I. INTRODUCTION: NEUTRON PRODUCTION SIMULATIONS**

Recently, three papers were published [1–3] on measuring the sizable neutron fluxes that were registered during thunderstorms. All three measurements were done at high altitudes<sup>1</sup> with neutron monitors [4] and thermal neutron counters. The Aragats and Tibet groups measure coinciding in time with neutrons gamma ray fluxes, although the Tibet group with a very high threshold of 40 MeV. Plastic scintillators (60 and 40 cm thick) were used to detect gamma rays. The Aragats and Tien-Shan groups, in addition to NMs, also used counters that were sensitive to neutrons (energy range of 0.025–1 eV). In all three experiments, the near surface electric field was monitored; at Tien-Shan and Mt. Aragats, the atmospheric discharges were monitored as well.

However, the three groups drastically differ in their explanations of the origin of neutron flux. The Tien-Shan group reports large fluxes of thermal neutrons correlated with atmospheric discharges; the Aragats and Tibet groups do not relate the neutron flux to lightning occurrences, but rather to photonuclear reactions of the bremsstrahlung gamma rays born in the relativistic runaway electron avalanches (RREA) [5] (also referred to as runaway breakdown [6]) in the thunderstorm atmospheres. However, the Tibet group assumes that gamma rays directly initiate NM counts by photonuclear reactions with lead producer of NM [3]; the Aragats group accepts the photonuclear reaction of the RREA gamma rays with the atmosphere as a source of neutrons [1].

The Tien-Shan group's hypothesis on the origin of neutrons is based on the large thermal neutron flux detected by an outdoor neutron detector correlated in time with

atmospheric discharges. To prove their claims, the Tibet and Aragats groups, along with presenting the measured neutron fluxes, also perform the Geant4 simulations to calculate the detector response. To resolve apparent ambiguity and to clarify neutron production mechanisms, we analyze in depth the simulation schemes used for predicting the neutron yield.

In Ref. [7], the neutron production was simulated by placing the “parent” photon source at heights of 5, 7.5, 10, 15, and 20 km in the atmosphere. Gamma ray energies were drawn from the bremsstrahlung spectrum initiated by the electrons in the atmosphere regions where electrical field is above the RREA threshold. For these heights and the used gamma ray spectrum, the neutron yield relative to gamma ray flux above the photonuclear reaction threshold ( $\sim 10$  MeV) was estimated to be  $\sim 0.6\%$ .

Reference [8] simulated a homogeneous gamma ray source in the form of a disk located at the fixed altitude. The gamma ray energy was simulated according to universal spectrum of bremsstrahlung photons initiated by the RREA electrons. The neutron yield relative to 10 MeV photon flux was estimated to be  $\sim 0.43\%$ . The authors conclude that most likely the photonuclear reactions in the air account for the neutron flux increases observed at mountain altitudes.

The model used by the Aragats group for neutron yield estimation was the same as described above. The relative yield of neutrons was estimated to be 0.3–0.6%, depending on the simulation conditions [1].

The simulations performed in Ref. [3] confirmed the above-mentioned estimates of relative neutron yield. By combining neutron and photon fluxes with an efficiency of NM to register gamma rays with energies above 10 MeV and neutrons above 1 keV (Fig. 1 of Ref. [3]), the Tibet group found that bremsstrahlung gamma rays interacting with lead producer of NM explained the signal obtained by the Tibet NM, and neutrons born in photonuclear

\*chili@aragats.am

<sup>1</sup>Aragats, 3200 m; Tien-Shan, 3340 m; Tibet, 4300 m.

reactions in the atmosphere give only a small fraction of the signal.

Additionally they conclude, “Consequently, not neutrons but gamma rays may possibly dominate enhancements detected by the Aragats neutron monitor (ANM).”

To check this statement and to decide on the nature of the detected peaks in the ANM, we perform a simulation of the RREA process in the strong electric field of the thunderstorm atmosphere. Instead of putting the gamma ray source on the fixed height, we direct simulate the RREA process using the seed electrons from the ambient cosmic ray population and follow the unleashed electron-gamma-ray avalanches till their attenuation. The electron and gamma ray content of RREA as well as neutrons born in the photonuclear reactions were traced till ground level. Also, we inject electrons not from one point but from an extended area. According to estimates done in Refs. [9,10] the gamma ray emitting area has dimensions of 600–700 m. The locality of the particle-emitting region is explained by the small sizes of the lower positive charge region (LPCR) [11] located on the base of the cloud. LPCR with a negatively charged region above it in the thundercloud constitutes the so-called lower dipole, which accelerates electrons downward. Therefore, the size of the particle-emitting region cannot be greater than the size of the LPCR.

From the survived particles’ rates we calculate the neutron and photon fluxes reaching the detector location on 3200 m asl. Due to much broader neutron angular distribution compared with the gamma ray one, the neutron relative yield will be a strictly increasing function of the distance from the projection of the center of radiation region in the thundercloud to the detector location (see Fig. 1). The bremsstrahlung gamma rays are producing

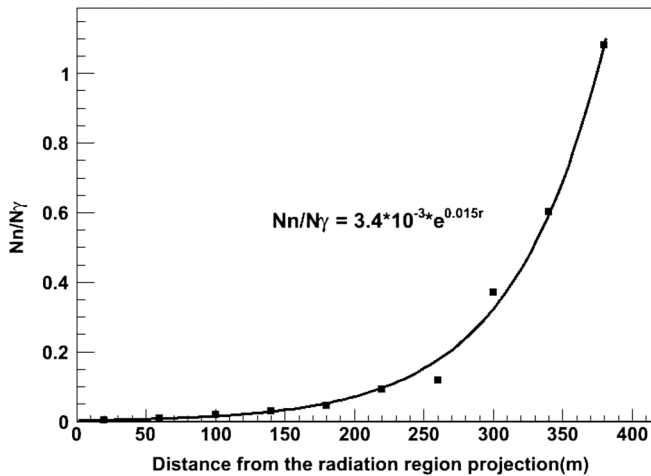


FIG. 1. Dependence of the neutron/gamma ray ratio on distance from the projection of the radiating region. Gamma rays are injected from an altitude of 4700 m according to energy spectrum measured during TGE on October 4, 2010. The detectors were located at 3200 m.

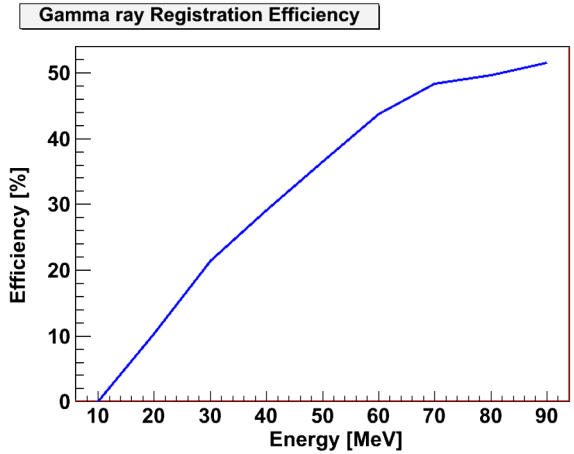


FIG. 2 (color online). The energy dependence of the photon detection efficiency by the 60-cm-thick scintillator.

in the narrow cones around vertically accelerated electrons; in contrast, neutrons emitted by the exciting nucleolus are distributed much broader.

## II. EXPLAINING NEUTRON MONITOR COUNTS: PHOTONUCLEAR REACTIONS IN THE AIR AND IN LEAD

To calculate the yield of neutrons from the photonuclear reactions of the gamma ray flux in lead, we need to recover the gamma ray flux fallen on the neutron monitor. The shape of the gamma ray flux will not differ significantly from the shape of the flux above the roof of the building, which we recovered and published in Ref. [12] for the two largest thunderstorm ground enhancements (TGEs) detected on September 19, 2009 and October 4, 2010 (see details in Refs. [13,14]). The energy dependence of the efficiency of gamma ray registration by the 60-cm-thick scintillator of the Aragats Solar Neutron Telescope is depicted in Fig. 2.

In Table I we demonstrate the bin-to-bin folding of the power law energy spectrum<sup>2</sup> with energy dependent efficiency acquired from Fig. 2. In the first column we depict the energy bin; in the second column we show the fraction of this particular bin relative to the energy range of 10–100 MeV; in the third column we show the efficiency of photon registration in this bin; in the last column we show the “folded” efficiency of the bin—the relative fraction multiplied to efficiency.

The aggregate folded efficiency of ASNT to register gamma ray flux fallen on the detector equals  $\sim 8\%$ ; we obtain this value by summing the “partial” efficiencies from the last column. Taking into account the registration efficiency and proceeding from the count rate enhancement of 10 280 per minute per  $m^2$  at the maximal flux minute as measured by ASNT on October 4, 2010, we come to

<sup>2</sup>For simplicity we assume the differential energy spectrum of gamma rays in the form of  $dN/dE \sim E^{-3}$ .

TABLE I. The efficiency of gamma ray registration by ASNT (gamma ray spectrum is adopted from Chilingarian *et al.*, 2012b,  $dN/dE \sim E^{-3}$ ).

Bin size [MeV]	Bin fraction [%]	Efficiency of registration [%]	“Folded” efficiency
10–20	75.00	4.83	0.0362
20–30	13.89	15.66	0.0217
30–40	4.86	25.58	0.0124
40–50	2.25	33.21	0.0074
50–60	1.22	40.11	0.0049
60–70	0.74	45.23	0.0033
70–80	0.48	48.76	0.0023
80–90	0.33	51.07	0.0016
90–100	0.23	51.94	0.0012

gamma ray flux incident the neutron monitor of  $10\,280/0.08 \sim 130\,000$  per minute per  $m^2$ . To estimate how many counts in NM this flux will generate, we adopt from Fig. 1 of Ref. [3] the energy dependence of the NM efficiency to detect photons. Analogically with Table I, we obtain partial efficiencies to register gamma rays (via generated in the lead neutrons) by NM; the details are depicted in Table II.

The aggregate efficiency of the registration of gamma rays obtained by summing the partial efficiencies depicted in the last column equals  $\sim 0.095\%$ . The expected NM count rate we obtain by multiplying the incident gamma ray flux on the aggregate detection efficiency  $130\,000 * 0.00095 \sim 120$  counts per minute per  $m^2$ , in good agreement with the measurement by the Aragats NM on October 4 (ANM) (see Table 2 of Ref. [1]).

The estimate of expected NM counts from another “super TGE” on September 19, 2009 [13] also proves hypothesis of neutron producing by photons in lead absorber. The number of additional gamma rays detected by ASNT on September 19 was 7452 per minute per  $m^2$ ; the recovered gamma ray flux above NM was  $7452/0.08 \sim 93\,000$  per minute per  $m^2$ ; the number of

TABLE II. The efficiency of gamma ray registration by neutron monitor (gamma ray spectrum is adopted from Chilingarian *et al.*, 2012b,  $dN/dE \sim E^{-3}$ ).

Bin size [MeV]	Bin fraction [%]	Efficiency of registration [%]	“Folded” efficiency
10–20	75.00	0.10	0.000750
20–30	13.89	0.09	0.000130
30–40	4.86	0.04	1.94E-05
40–50	2.25	0.08	0.000018
50–60	1.22	0.09	0.000011
60–70	0.74	0.10	7.37E-06
70–80	0.48	0.10	4.78E-06
80–90	0.33	0.10	3.28E-06
90–100	0.23	0.10	3.28E-06

expected ANM was  $93\,000 * 0.00095 \sim 88$  counts per minute per  $m^2$ , compatible with what was measured in the experiment.

However, from Table 2 of Ref. [1] we see that only for these two “super events,” the large intensity of gamma rays can generate in lead enough neutrons to explain the detected NM count rate. For rest 10 smaller by gamma ray content events the neutron yield will be too small to explain the additional NM counts by the direct gamma rays’ interactions with lead producer of NM. If we again look at Fig. 1, we can see that small neutron/gamma ray ratios and corresponding large gamma ray fluxes can occur infrequently when the radiating region is just above the detector. At any offset of the detector location related to the radiated region in the thundercloud, the gamma ray content will quickly diminish. In contrast, the neutron content due to a much broader angular distribution will remain more or less constant on much larger distances. Therefore, we can expect that the neutron content on large distances can reach several tens of percent of detected gamma ray flux, and if the radiation region is far from the detector location site we can detect only neutrons without gamma ray contribution. This category of neutron events (much more abundant compared with the “large gamma” events considered above) can be explained by the photonuclear reactions of gamma rays in the atmosphere. For the ten “small” events from Table 2 of Ref. [1], we can estimate that the neutron/gamma ray ratio is equal to  $\sim 5\text{--}15\%$ , which is rather probable from pure geometrical consideration. We do not recover gamma ray intensity for the small events due to the scarcity of the energy deposit histograms measured by the 60-cm-thick scintillator. However, we can roughly estimate this intensity by considering the count rates and recovered intensities of the two largest events. The numbers of counts and recovered intensities above the roof of a building for the September 19, 2009 and October 4, 2010 events are correspondingly, 7452–104 000 and 10 280 and 153 000 per minute per  $m^2$ . The ratio of recovered/detected is 14 and 14.9, and the mean is 14.5. By the analogy, we can estimate the intensity of the May 21, 2009 event’s registered gamma ray enhancement of 1920 as  $1920 * 14.5 = 27\,840$  gamma rays per minute per  $m^2$ . If we assume a neutron/gamma ray ratio of 10%, we will have 2784 neutrons above the roof of the building, and proceeding from the aggregate efficiency of detecting photonuclear neutron spectra estimated to be 2.4%, we come to expect neutron monitor counts of 67 per minute per  $m^2$ , which is in good agreement with the 83 counts per minute per  $m^2$  measured by ANM.

### III. CHECK OF HYPOTHESIS ON THERMAL NEUTRON FLUXES

Reference [2] reported the registration of intensive fluxes of low-energy neutrons generated during thunderstorms. The authors connect registered neutron fluxes with

atmospheric discharges. Unfortunately, the empirical data on neutron detector count rates were not supported by the detector response calculation and with a model of neutron generation. Only several episodes of the detected one-minute count rate enhancements that were possibly correlated in time with the lightning occurrences were presented. Reported observations were done with the Tien-Shan 18NM64 neutron monitor (TSNM) and thermal neutron counters (TSNC) located outdoors and indoors, respectively (see Fig. 2 in Ref. [15]). The counters were filled with  $\text{He}^3$  gas. Because of the absence of producing and moderating material, these counters can register effectively only neutrons having energies in the range of 0.01–1 eV Gurevich *et al.*, 2012. On August 20, 2010 at 12:54, 12:56, 12:58, 13:00, and on August 10, 2010 at 8:06 and 8:08 the external counters register the following enhancements [2]: 1558, 720, 758, 2055, 1673, and 1225 per minute. The same type of TSNM counters located indoors (internal) register the following enhancements: 641, 418, 323, 716, 927, and 922 per minute, i.e., 35–75% of the outdoor (external) counters.

Neutron fluxes fell on the roof of the building where the TSNM and indoor (internal) TSNC were located. The building roof matter was comprised of 2 mm iron tilt, 20 cm carbon [2], and 2.5 cm wood. The Geant4 simulations of the neutron transport through the roof material demonstrated that only 7% (compared with 35–75% calculated above) of the thermal neutron flux can penetrate the roof.

To compare the reported TSNM counts with those expected from the detector response calculation, we have to recover the intensity of thermal neutrons that fell on the roof. A product of the registration efficiency and the total area of six helium counters is  $0.45 \text{ m}^2$  [15]. Accordingly, we readily obtain the flux of thermal neutrons for six considered neutron events: 3462, 1600, 1684, 4567, 3717, and 2722 neutrons per  $\text{m}^2$  per minute. Assuming 0.5% efficiency [2] of TSNM to detect thermal neutrons, we cannot expect more than 40 counts of the TSNM for all six neutron events. However, the TSNM counts reported in Ref. [2] are 804, 1136, 913, 587, 2821, and 2112 per minute.

We can assume that along with thermal neutron flux there is also a flux of neutrons born in photonuclear reaction in the thunderstorm atmosphere not detected by the outdoor TSNC. To date, the maximal estimated neutron flux at Mt. Aragats is  $\sim 5000$  neutrons per  $\text{m}^2$  per minute. By considering the higher location of Tien-Shan we can double this number and assume that photonuclear neutron flux at Tien-Shan can reach 10000 neutrons per  $\text{m}^2$  per minute. Geant4 simulations demonstrate that only  $\sim 20\%$  of photonuclear neutrons can penetrate the roof material; additionally, the 20-cm-thick carbon layer effectively thermalized neutrons, and 97% of the initial neutrons incident on the indoor detectors will be thermalized.

Therefore, 2000 (20% of 10000) neutrons per minute per  $\text{m}^2$  falling on the indoor TSNM will generate approximately the same number of counts (40 per minute per  $\text{m}^2$ ) as the thermal neutron flux. Thus, the hypothesis of the photonuclear nature of neutron flux in Tien-Shan also cannot explain the reported count rate enhancements. Measured by the outdoor TSNC, thermal neutron flux should be five to ten times more intensive to explain the TSNC counts and 20–50 times more intensive to explain the TSNM counts.

#### IV. SIMULTANEOUS DETECTION OF CHARGED AND NEUTRAL FLUXES BY NOR AMBERD DETECTOR ASSEMBLY

New experimental evidence on neutron production correlated with thunderstorms originates from another experimental setup located on the slopes of Mt. Aragats at the Nor Amberd research station. The experimental facilities located at Nor Amberd operated as a part of the Aragats Space Environmental Center [16] and measure fluxes of gamma rays, thermal and high-energy neutrons, and high-energy muons; we consider the registration of multiple particle fluxes as an absolutely necessary condition for making physical inference on the neutron origin.

Detector assemblies measuring secondary cosmic ray fluxes that originated from protons and ions accelerated on the Sun and in the Galaxy are located on the slopes of Mt. Aragats at the Nor Amberd research station at 2000 m above sea level. The Nor Amberd detecting system consists of an 18NM64 neutron monitor (NANM) with three sections of six neutron counters in each, and a multidirectional muon monitor (NAMMM) with two layers of 5-cm-thick plastic scintillators overviewed by a photomultiplier above and below two sections of NANM. Also included are two proportional counters without a lead producer and a polyethylene moderator for detecting thermal neutrons (see Fig. 3). The energy threshold of the upper scintillators is determined by the roof matter and by data acquisition electronics and equals  $\sim 10$  MeV. The upper scintillator registered charged flux above the threshold with very high efficiency reaching 99%; however, the 5-cm plastic scintillator also registers neutral flux (gamma rays and neutrons) although with much smaller efficiency of  $\sim 5$ –10%. The bottom layer of scintillators is located under a significant amount of matter including 10 cm of lead and its energy threshold is  $\sim 350$  MeV; therefore, the bottom layer measures mostly high-energy muons.

Data acquisition electronics calculates all possible coincidences of the upper and bottom scintillators for both sections of the NAMMM. By counting the coincidences of upper and bottom scintillators it is possible to monitor muon fluxes for 12 incident directions. The NANM operates with three dead times ranging from 0.4 to 1250  $\mu\text{s}$ . The monitor counts with shortest dead time give possibility

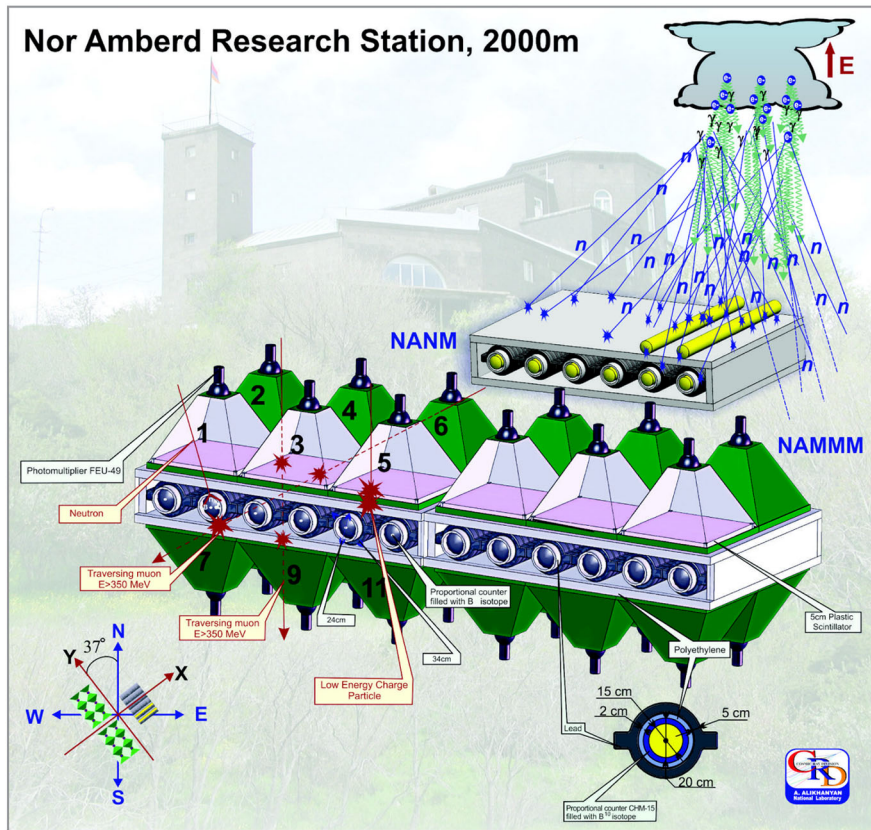


FIG. 3 (color online). Nor Amberd multidirectional muon monitor arranged above and below two sections of the Nor Amberd Neutron Monitor; “bare” proportional counters are located on the third section of NANM.

to count almost all thermal neutrons entering the sensitive volume of the proportional chamber; the long dead time provides a one-to-one relation between the counts and the high energy atmospheric hadrons incident on the detector. If neutron bursts are incident on detector the shortest dead time will provide a registration of almost all neutrons; the longer dead time will miss additional neutrons coming simultaneously within 1250  $\mu$ s.

In Fig. 4 we post the measured enhancements of time series taken on March 28, 2009 of one-minute count rates of NAMMM top (mostly gamma rays) and bottom layers (mostly muons) as well as NANM one-minute time series corresponding to shortest dead time.

The statistical accuracy of the measurements and significances of the detected peaks are posted in Table III. In Fig. 4 we see a large enhancement of the counts in the upper layer of NAMMM conditioned in the absence of a signal in the lower layer (combination 10—a signal in the upper layer and no signals in the bottom layer of the scintillators); a significant enhancement of the count rate of the neutron monitor and a depletion of counts of high-energy muons. The deficit of muons measured simultaneously with an enhancement of gamma rays is one of the characteristics of the so-called TGEs (see details in Ref. [12]).

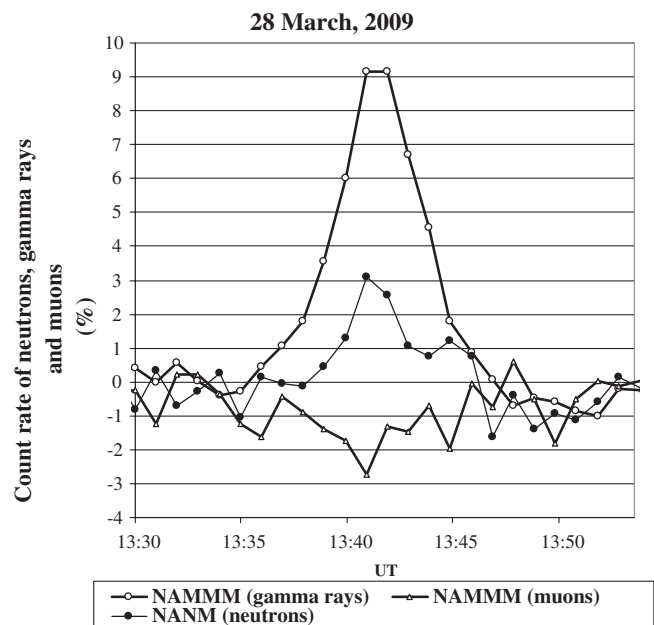


FIG. 4. The one-minute time series of count rates of upper and top layers of NANM and NAMMM.

TABLE III. Statistical characteristics of detectors and detected peaks and dips on March 28, 2009 at 13:43.

Detector	Mean count rate per minute	Standard deviation-SD ( $\sigma$ ) and relative standard deviation	Percent of enhancement	Number of SD ( $\sigma$ ) in peak	Number of additional particles (or deficit for muons) at minute of maximal excess ( $\text{min}^{-1} \text{m}^{-2}$ )
NANM neutrons	30000	300 (1%)	3.2%	$3.2\sigma$	53
NAMMM upper (10)	121150	348 (0.29%)	9.2%	$32\sigma$	924
NAMMM (muons $> 350$ MeV); vertical direction excluded	24000	155 (0.65%)	-2, 2%	$3.5\sigma$	-45

## V. POSSIBLE SYSTEMATIC ERRORS

The assumed in the simulations charge structure of the thundercloud (strengths and elongations of the electric field, cloud height, and size of the radiating region); although they are in good agreement with rare *in situ* measurements they, can significantly deviate from the conditions of the Aragats thunderstorms, which give rise to detected TGE events. We do not measure the elongation and strength of the electrical field in the particular thundercloud. We also do not directly measure the size of the radiation region in the thundercloud. Therefore, the obtained estimates of the neutron-to-gamma-ray ratio give us overall understanding of the neutron generation process and dependence on the parameters that we cannot locate yet (distance to and geometry of the radiation region).

Estimating the neutron monitor efficiency for low-energy neutrons ( $> 1$  keV) and photons ( $> 10$  MeV) by simulations with Geant4 code is rather difficult due to very small values of efficiencies ( $\sim 0.1$ –2%).

In our Geant4 simulations of the Tien-Shan detectors response we used known from publications detector setup. However, it possibly changed from the published one during the experiment. Additional calculations are needed (better by the Tien-Shan group) to finally understand the measurements presented in Ref. [2].

## VI. CONCLUSIONS

We analyzed the data on recently reported neutron fluxes correlated with thunderstorms. The Tibet group explained the detected count rate enhancement in the neutron monitor by the previously neglected direct registration of gamma ray photons by NM. According to their estimates, the photonuclear reactions of gamma rays in

lead producer of NM exceed the contribution of the neutrons born in the photonuclear reactions in the atmosphere. The Aragats group supported another hypothesis of the neutron production in the photonuclear reactions in the atmosphere.

A new realistic simulation of the RREA process in the thunderstorm atmosphere checked the situation. We found that the explanation of the Tibet group is supported by a new simulation if the radiation region is just above the neutron detector. At any offset of the radiation region relative to the detector location, the contribution to the NM counts of direct gamma ray interactions in a lead absorber quickly diminished and the “atmospheric” neutron contribution enlarged.

Therefore, both photonuclear processes in the air and in the lead absorber of NM should be considered to explain the neutron fluxes correlated with thunderstorms.

Also, we find that the simulations of neutron yield with gamma ray source located on the fixed altitude above the detector gives optimistically biased relative neutron yield. Proceeding from the thermal neutron count rates measured by the outdoor thermal neutron counter reported in Ref. [2], we calculate the expected counts of the indoor Tien-Shan neutron monitor and the indoor thermal neutron counter taking into account the detector response. The calculated fluxes of the indoor detectors are much lower than the reported ones. Thus, the reported data on indoor and outdoor detectors are not consistent.

The Aragats and Tibet measurements do not support the hypothesis of particle fluxes directly related to the atmospheric discharges, accepted by the Tien-Shan group. Accordingly, during the developed lower positive charge region in the thundercloud (necessary condition of the creation of lower dipole accelerated electrons downward), the flash rate is quite low [11,17].

[1] A. Chilingarian, N. Bostanjyan, and L. Vanyan, *Phys. Rev. D* **85**, 085017 (2012).

[2] A. V. Gurevich, V. P. Antonova, A. P. Chubenko, A. N. Karashtin, G. G. Mitko, M. O. Ptitsyn, V. A. Ryabov,

A. L. Shepetov, Y. V. Shlyugaev, L. I. Vildanova, and K. P. Zybin, *Phys. Rev. Lett.* **108**, 125001 (2012).

[3] H. Tsuchiya, K. Hibino, K. Kawata *et al.*, *Phys. Rev. D* **85**, 092006 (2012).

- [4] C.J. Hatton and H. Carmichel, *Can. J. Phys.* **42**, 2443 (1964).
- [5] L.P. Babich, I.M. Kutsyk, E.N. Donskoy, and A.Y. Kudryavtsev, *Phys. Lett. A* **245**, 460 (1998).
- [6] A.V. Gurevich, G.M. Milikh, and R.A. Roussel-Dupre, *Phys. Lett. A* **165**, 463 (1992).
- [7] B.E. Carlson, N.G. Lehtinen, and U.S. Inan, *J. Geophys. Res.* **115**, a00e19 (2010).
- [8] L.P. Babich, E.I. Bochkov, I.M. Kutsyk, and R.A. Roussel-Dupre, *J. Geophys. Res.* **115**, A00E28 (2010).
- [9] H. Tsuchiya *et al.*, *J. Geophys. Res.* **116**, D09113 (2011).
- [10] T. Torii, T. Sugita, M. Kamogawa, Y. Watanabe, and K. Kusunoki, *Geophys. Res. Lett.* **38**, L24801 (2011).
- [11] A. Chilingarian and R. Mkrtychyan, *Phys. Rev. D* **86**, 072003 (2012).
- [12] A. Chilingarian, B. Mailyan, and L. Vanyan, *Atmos. Res.* **114–115**, 1 (2012).
- [13] A. Chilingarian, A. Daryan, K. Arakelyan, A. Hovhannisyan, B. Mailyan, L. Melkumyan, G. Hovsepyan, S. Chilingaryan, A. Reymers, and L. Vanyan, *Phys. Rev. D* **82**, 043009 (2010).
- [14] A. Chilingarian, G. Hovsepyan, and A. Hovhannisyan, *Phys. Rev. D* **83**, 062001 (2011).
- [15] A.P. Chubenko, A.L. Shepetov, V.P. Antonova, P.A. Chubenko, and S.V. Kryukov, *J. Phys. G* **35**, 085202 (2008).
- [16] A. Chilingarian *et al.*, *Nucl. Instrum. Methods Phys. Res., Sect. A* **543**, 483 (2005).
- [17] X. Qie, T. Zhang, G. Zhang, T. Zhang, and X. Kong, *Atmos. Res.* **91**, 244 (2009).